

470 **Supplementary material**



471

472

*Geophysical Research Letters*

473

Supporting Information for

474 **Variability of snow and rainfall partitioning into evapotranspiration and summer runoff**

475

**across nine mountainous catchments**

476 Matthias Sprenger<sup>1\*</sup>, Rosemary W.H. Carroll<sup>2</sup>, James Dennedy-Frank<sup>1</sup>, Erica R. Siirila-Woodburn<sup>1</sup>,

477 Michelle E. Newcomer<sup>1</sup>, Wendy Brown<sup>3</sup>, Alexander Newman<sup>3</sup>, Curtis Beutler<sup>3</sup>, Markus Bill<sup>1</sup>, Susan

478

S. Hubbard<sup>4</sup>, Kenneth H. Williams<sup>1,3</sup>

479

<sup>1</sup>Lawrence Berkeley National Laboratory, Berkeley, CA, USA

480

<sup>2</sup>Desert Research Institute, Reno, NV, USA

481

<sup>3</sup>Rocky Mountain Biological Laboratory, Crested Butte, CO, USA

482

<sup>4</sup>Oak Ridge National Laboratory, Oak Ridge, TN, USA

483

484 **Contents of this file**

485 Text S1: Gap filling of streamflow data

486 Text S2: References for supplementary information

487 Suppl. Fig. 1 Cross-correlation of different catchment characteristics. TWI = Topographic wetness

488 index [-]; DD\_km\_km2 = Drainage density [km km<sup>-2</sup>]; Mancos = share of surface area with

489 Mancos shale geology [%]; Barren = share of surface area with bare soil or rock [%]. Bold and

490 black numbers represent significant correlations at p<0.05 and bold grey numbers for p<0.10.. 27

491 Suppl. Fig. 2 Correlation between the four components of rotated principle component analysis  
492 and their correlation with various catchment characteristics (same as in Suppl. Fig. 1. From these  
493 relationships, we chose four characteristics that represent the four components: Tree density,  
494 aspect, size area, and drainage density. Bold and black numbers represent significant correlations  
495 at  $p < 0.05$  and bold grey numbers for  $p < 0.10$ . ..... 28

496 Suppl. Fig. 3 Distribution of  $\delta^{18}\text{O}$  values for snow ( $\delta^{18}\text{O}_{\text{PS}}$ ) and rain ( $\delta^{18}\text{O}_{\text{PR}}$ ) samples taken during  
497 water year 2015 and 2016 at the location shown in Figure 1. Lines show the kernel density estimate  
498 for both histograms. Vertical values represent the weighted average values for snow and rain,  
499 respectively. .... 29

500 Suppl. Fig. 4 Upper panel: Snow water equivalent (SWE) measured at the SNOTEL site in  
501 Schofield (location shown in Figure 1), Rainfall ( $P_{\text{R}}$ ) and snowfall ( $P_{\text{S}}$ ) hourly sums for the East  
502 River catchment defined by the Pumphouse outlet (location shown in Figure 1). Lower panel:  
503 Measured discharge ( $Q$ ) and  $\delta^{18}\text{O}$  values for water sampled during the summer ( $\delta^{18}\text{O}_{\text{S}}$ ) and non-  
504 summer ( $\delta^{18}\text{O}_{\text{NS}}$ ) periods at the Pumphouse. .... 30

505 Suppl. Fig. 5 Same as in Suppl. Fig. 4, but for the Rustlers Creek catchment. .... 31

506 Suppl. Fig. 6 Same as in Suppl. Fig. 4, but for the Rock Creek catchment. .... 31

507 Suppl. Fig. 7 Same as in Suppl. Fig. 4, but for the Quigley Creek catchment. .... 32

508 Suppl. Fig. 8 Same as in Suppl. Fig. 4, but for the East River catchment below Copper Creek  
509 tributary. .... 32

510 Suppl. Fig. 9 Same as in Suppl. Fig. 4, but for the East River catchment above the Quigley  
511 tributary. .... 33

512 Suppl. Fig. 10 Same as in Suppl. Fig. 4, but for the Copper Creek catchment. .... 33

513 Suppl. Fig. 11 Same as in Suppl. Fig. 4, but for the Coal Creek catchment. .... 34

514 Suppl. Fig. 12 Same as in Suppl. Fig. 4, but for the Bradley Creek catchment. .... 34

515 Suppl. Fig. 13 Long-term (2015-2020) isotope mass balance for the nine catchments. Snow ( $P_{\text{S}}$ )  
516 and rain ( $P_{\text{R}}$ ) are split into evapotranspiration (ET), non-summer ( $Q_{\text{NS}}$ ) and summer season  
517 discharge ( $Q_{\text{S}}$ ) based on endmember splitting analysis. The composition of ET,  $Q_{\text{NS}}$  and  $Q_{\text{S}}$  with  
518 regard to snow and rain is based on endmember mixing analysis. .... 35

519

520 Suppl. Table 1 Catchment specific characteristics: total surface area [km<sup>2</sup>], catchment scale  
521 averages of the slope [-], aspect [°], elevation [m a.s.l.], relief [m], drainage density [km/km<sup>2</sup>],  
522 topographic wetness index (TWI) [-], share of montane, subalpine, upper subalpine, alpine,  
523 Mancos lithology, and barren land as % of total catchment area. EAQ = East River above Quigley,  
524 EBC = East River above Copper Creek, PH = Pumphouse. We derived catchment average tree  
525 cover density using USGS Landfire at 30 m raster maps (Landfire, 2008) weighing the different  
526 forest classes by their given tree density. Alpine > 3750 m; upper subalpine: 3700-3525 m;  
527 subalpine: 3525–3000 m, montane: <3000 m..... 36  
528

529 **Text S1: Gap filling of streamflow data**

530 We used a random forest ensemble machine learning algorithm to regress hourly discharge ( $Q$ ,  
531 m<sup>3</sup>/s) between nearby discharge monitoring stations within the East River watershed network  
532 (Shortridge et al., 2016; Dwivedi et al. 2022). This method included stations monitored by the  
533 USGS from 1940-2021. All sites have some periods where major gaps exist. Hourly discharge data  
534 for long term USGS monitoring stations (Almont Station ID# 09112500, East River Below Cement  
535 Creek Station ID# 09112200, and Gunnison Station ID# 09114500) were obtained from the USGS  
536 NWIS portal using the R dataRetrieval package (Hirsch & De Cicco, 2015; USGS, 2022) and this  
537 data was merged with East River discharge monitoring locations (Carroll and Williams, 2019;  
538 Carroll et al. 2021). The machine learning algorithm within the R package randomForest  
539 implements Breiman's random forest algorithm for classification and regression (Breiman, 2001;  
540 Liaw & Wiener, 2018). We selected random forest because of the robust capabilities to handle a  
541 large number of predictor and target variables, and handle the broad temporal structure of the data  
542 (hourly over 8 years). In our approach, we allowed all available continuous discharge from any  
543 station to be used as predictor variables for the target variable (discharge station with gaps) (Jain  
544 et al., 2020). Once discharge was simulated based on a stations neighbors, we filled in the gap with  
545 the simulated values thus preserving all of the original data and the temporal structure.  
546 Additionally, this method preserves the presence of any non-stationarity within the data. Gap-filled  
547 discharge data are freely and publically available on ESS-DIVE (Newcomer et al. 2022)  
548

549 **Text S2: References for supplementary information**

550 Breiman, L. (2001). Random Forests. *Machine Learning*, 45(1), 5–32.  
551 <https://doi.org/10.1023/A:1010933404324>

552 Carroll R ; Williams K (2019): Discharge data collected within the East River for the Lawrence  
553 Berkeley National Laboratory Watershed Function Science Focus Area (water years  
554 2015-2018). Watershed Function SFA, ESS-DIVE repository. Dataset.  
555 doi:10.21952/WTR/1495380.

556 Carroll R ; Newman A ; Beutler C ; Williams K (2021): Stream discharge data collected within  
557 the East River, Colorado for the Lawrence Berkeley National Laboratory Watershed  
558 Function Science Focus Area (water years 2019 to 2020). Watershed Function SFA, ESS-  
559 DIVE repository. Dataset. doi:10.15485/1779721.

560 Dwivedi, D., Mital, U., Faybishenko, B., Dafflon, B., Varadharajan, C., Agarwal, D., et al.  
561 (2021). Imputation of Contiguous Gaps and Extremes of Subhourly Groundwater Time  
562 Series Using Random Forests. *Journal of Machine Learning for Modeling and*  
563 *Computing*. <https://doi.org/10.1615/JMachLearnModelComput.2021038774>

564 Hirsch, R. M., & De Cicco, L. (2015). User guide to Exploration and Graphics for RivEr Trends  
565 (EGRET) and dataRetrieval: R packages for hydrologic data (version 2.0, February  
566 2015). Retrieved from <https://dx.doi.org/10.3133/tm4A10>

567 Jain, P., Coogan, S. C. P., Subramanian, S. G., Crowley, M., Taylor, S., & Flannigan, M. D.  
568 (2020). A review of machine learning applications in wildfire science and management.  
569 *Environmental Reviews*, 28(4), 478–505. <https://doi.org/10.1139/er-2020-0019>

570 Liaw, A., & Wiener, M. (2018). Breiman and Cutler’s Random Forests for Classification and  
571 Regression. CRAN. Retrieved from  
572 <https://www.stat.berkeley.edu/~breiman/RandomForests/>

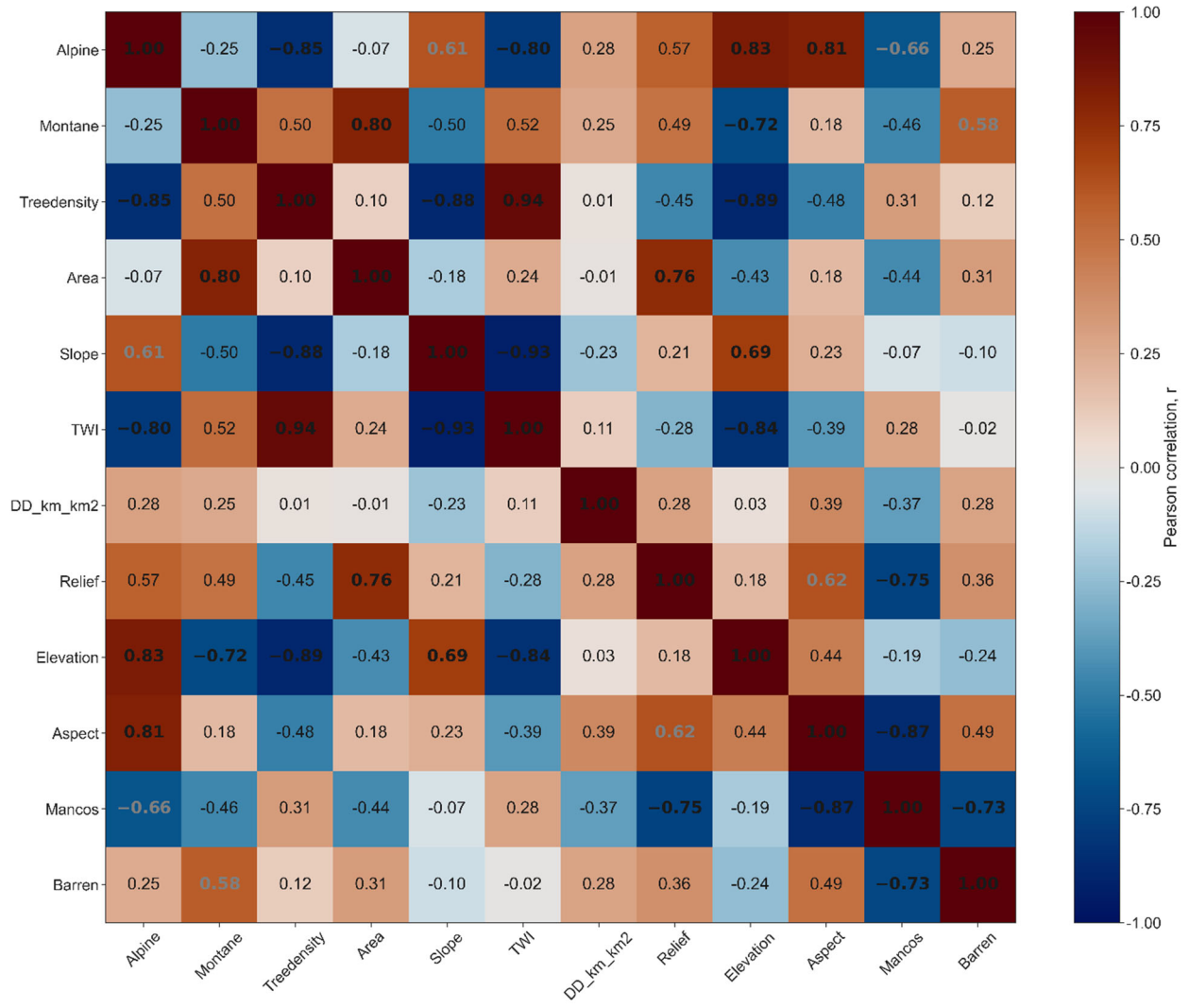
573 Newcomer, M.E., Williams, K.W., and Carroll R.W.H. (2022). Machine Learning Assisted Gap-  
574 Filled Discharge Data for the East River Community Watereshed for Water Years 2014-  
575 2021. [Data set]. Environmental System Science Data Infrastructure for a Virtual  
576 Ecosystem; Watershed Function SFA.  
577 [https://www.dropbox.com/s/gd9jxv4flx7blao/All\\_RF\\_Wide.csv?dl=0](https://www.dropbox.com/s/gd9jxv4flx7blao/All_RF_Wide.csv?dl=0) (Upload to

578 <https://ess-dive.lbl.gov/> in progress and DOI fill follow)

579 Shortridge, J. E., Guikema, S. D., & Zaitchik, B. F. (2016). Machine learning methods for  
580 empirical streamflow simulation: a comparison of model accuracy, interpretability, and  
581 uncertainty in seasonal watersheds. *Hydrology and Earth System Sciences*, 20(7), 2611–  
582 2628. <https://doi.org/10.5194/hess-20-2611-2016>

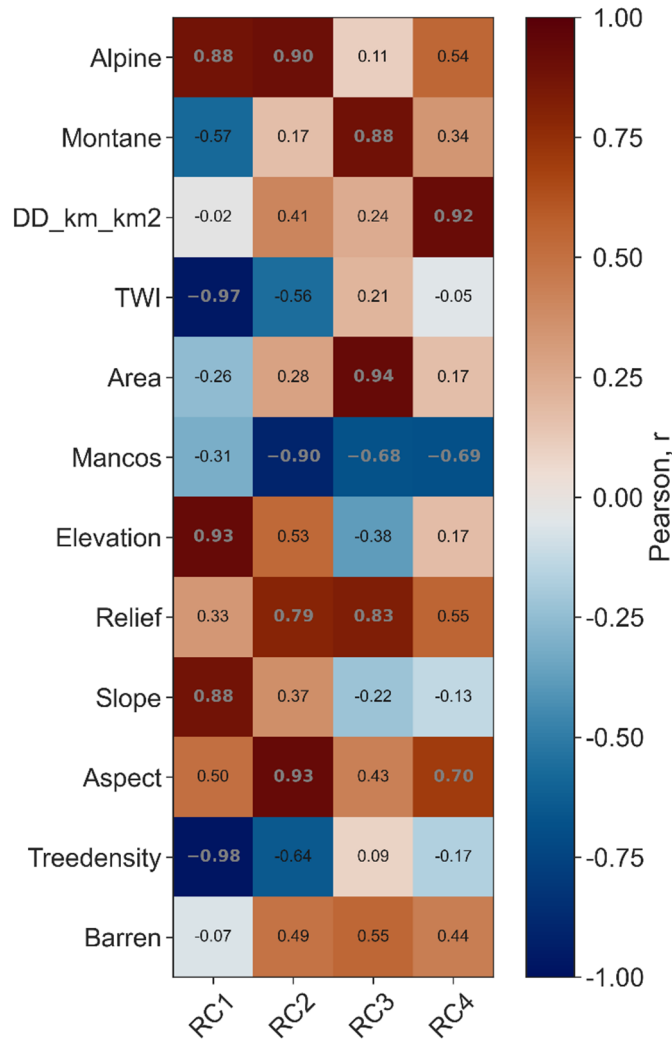
583 USGS. (2022). National Water Information System-Web Interface. Retrieved from  
584 <https://waterdata.usgs.gov/nwis>

585



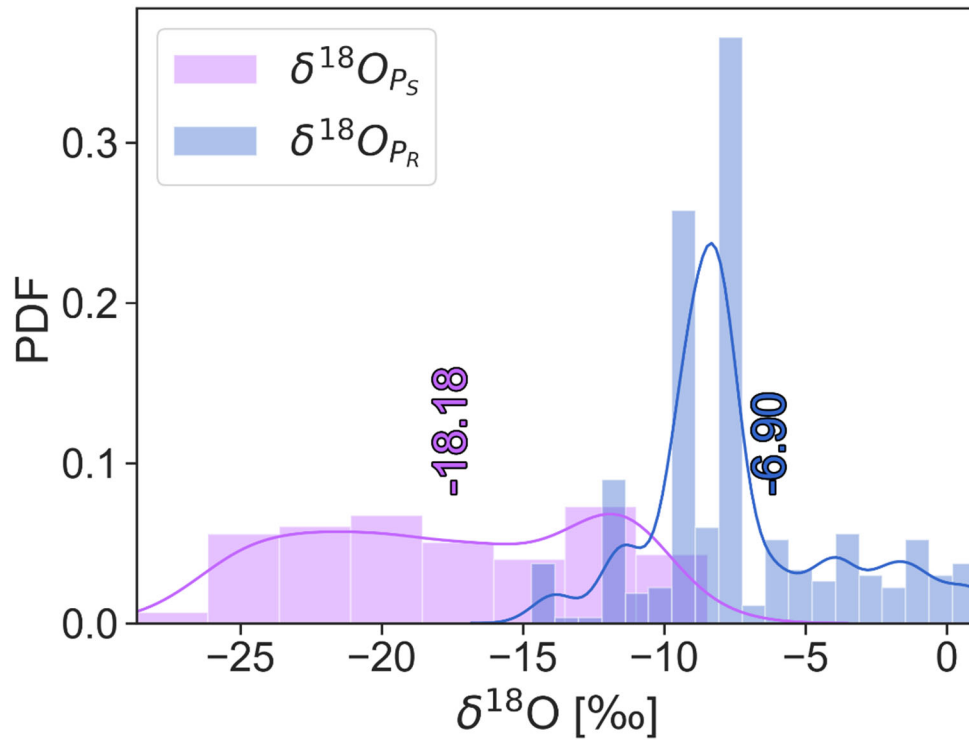
586

587 *Suppl. Fig. 1 Cross-correlation of different catchment characteristics. TWI = Topographic*  
 588 *wetness index [-]; DD\_km\_km2 = Drainage density [km km<sup>-2</sup>]; Mancos = share of surface area*  
 589 *with Mancos shale geology [%]; Barren = share of surface area with bare soil or rock [%]. Bold*  
 590 *and black numbers represent significant correlations at p<0.05 and bold grey numbers for p<0.10.*



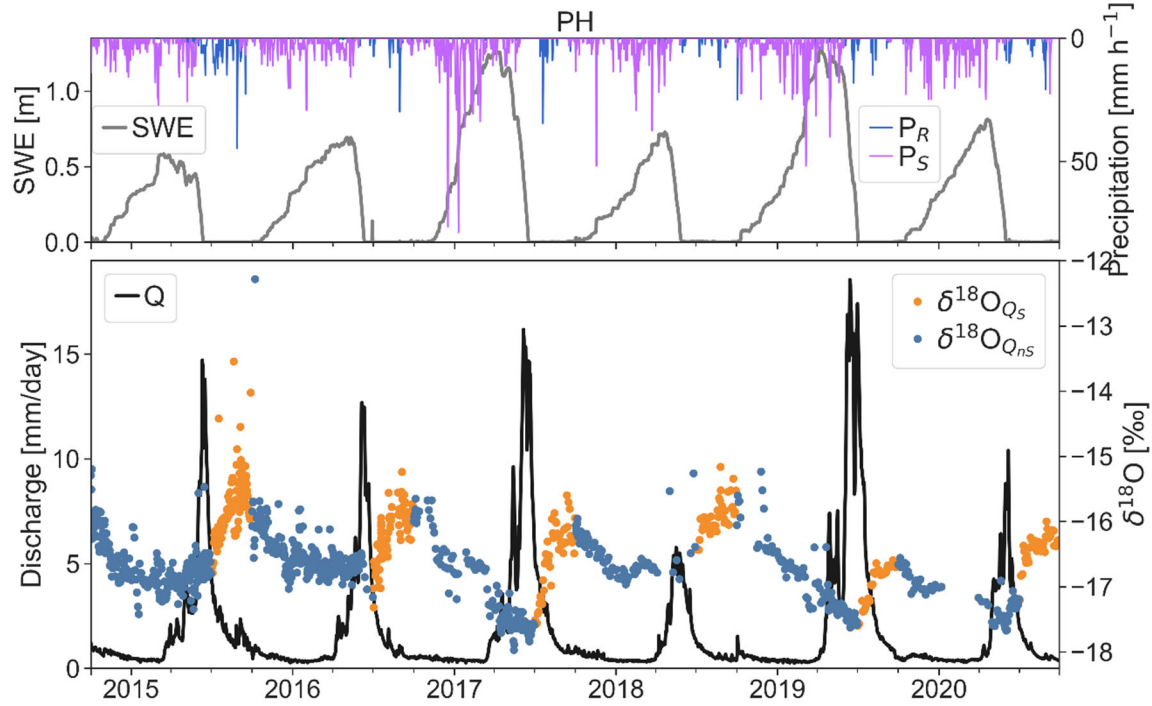
591

592 *Suppl. Fig. 2 Correlation between the four components of rotated principle component analysis*  
 593 *and their correlation with various catchment characteristics (same as in Suppl. Fig. 1). From these*  
 594 *relationships, we chose four characteristics that represent the four components: Tree density,*  
 595 *aspect, size area, and drainage density. Bold and black numbers represent significant correlations*  
 596 *at  $p < 0.05$  and bold grey numbers for  $p < 0.10$ .*



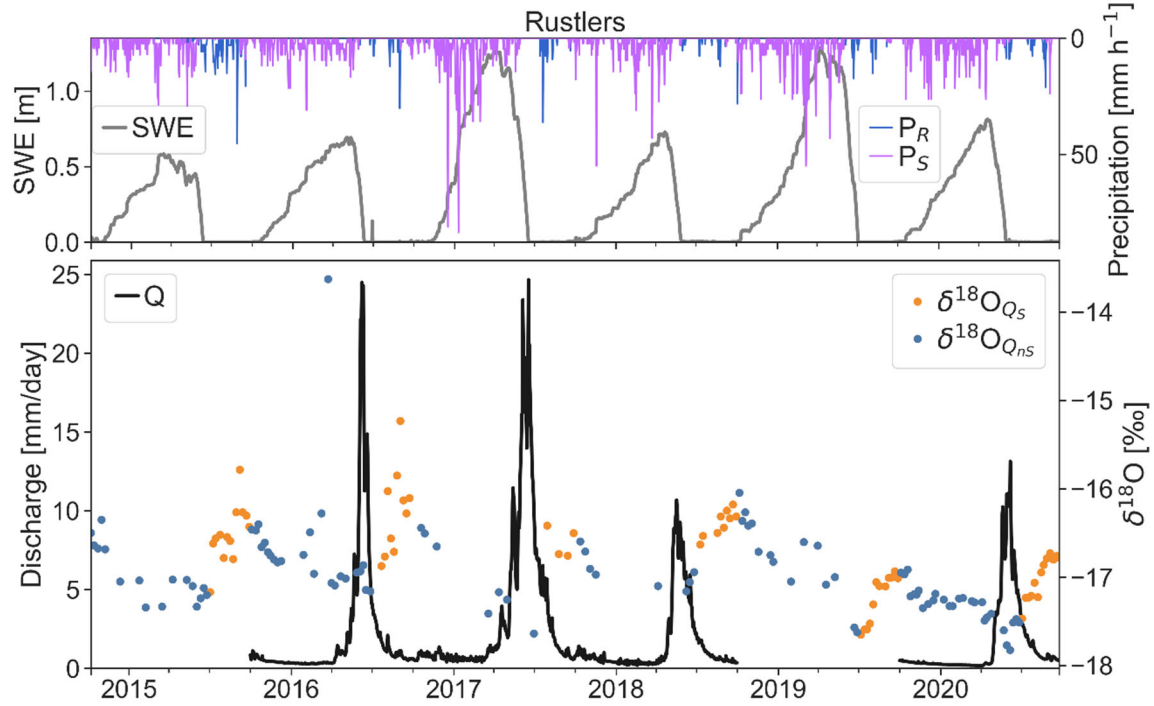
597

598 *Suppl. Fig. 3 Distribution of  $\delta^{18}\text{O}$  values for snow ( $\delta^{18}\text{O}_{P_S}$ ) and rain ( $\delta^{18}\text{O}_{P_R}$ ) samples taken during*  
 599 *water year 2015 and 2016 at the location shown in Figure 1. Lines show the kernel density estimate*  
 600 *for both histograms. Vertical values represent the weighted average values for snow and rain,*  
 601 *respectively.*



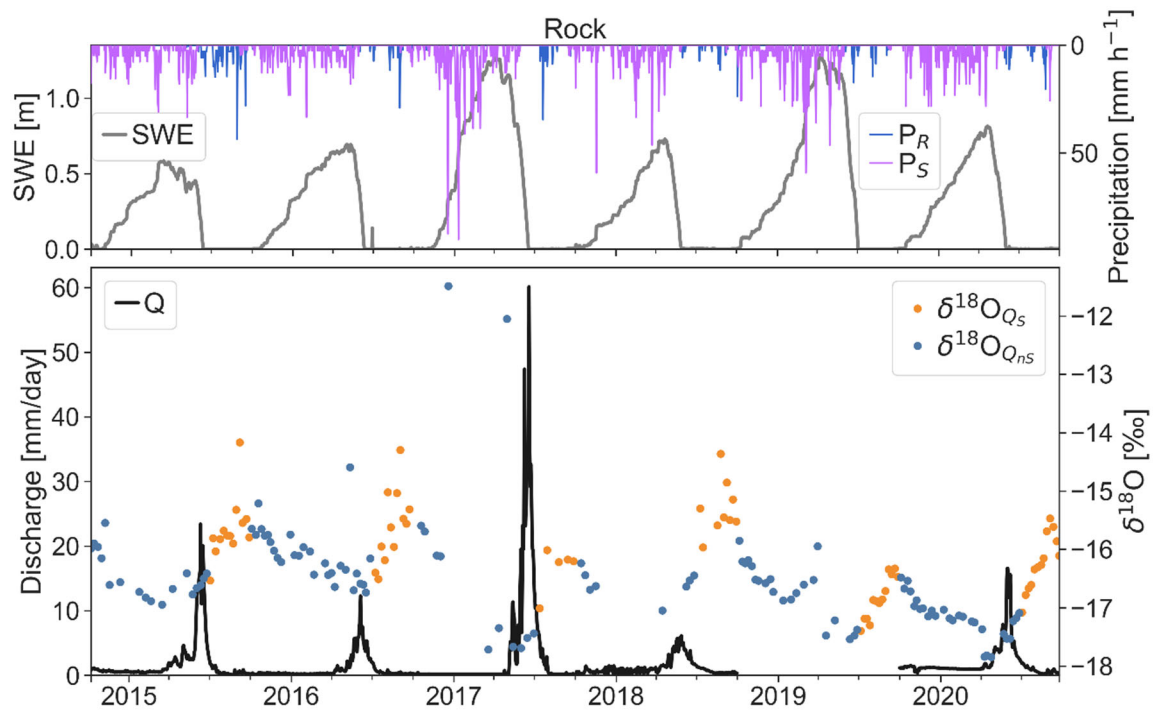
602

603 *Suppl. Fig. 4 Upper panel: Snow water equivalent (SWE) measured at the SNOTEL site in*  
 604 *Schofield (location shown in Figure 1), Rainfall ( $P_R$ ) and snowfall ( $P_S$ ) hourly sums for the East*  
 605 *River catchment defined by the Pumphouse outlet (location shown in Figure 1). Lower panel:*  
 606 *Measured discharge ( $Q$ ) and  $\delta^{18}O$  values for water sampled during the summer ( $\delta^{18}O_S$ ) and non-*  
 607 *summer ( $\delta^{18}O_{NS}$ ) periods at the Pumphouse.*



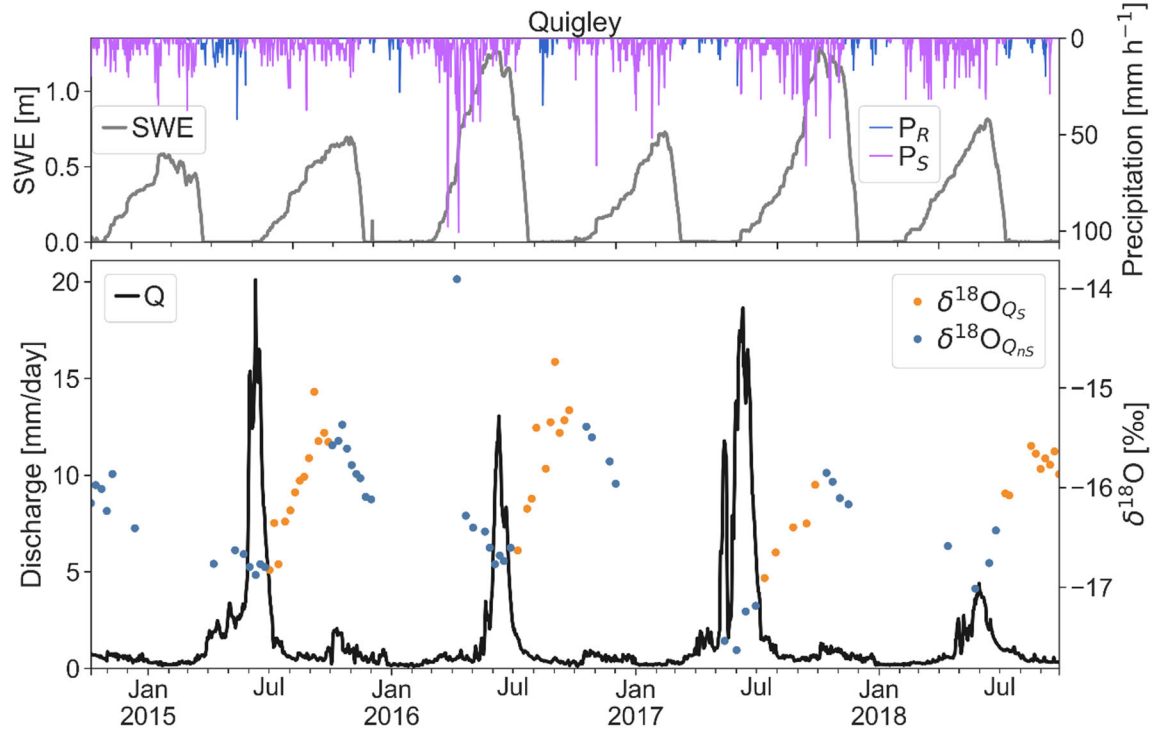
608

609 *Suppl. Fig. 5 Same as in Suppl. Fig. 4, but for the Rustlers Creek catchment.*



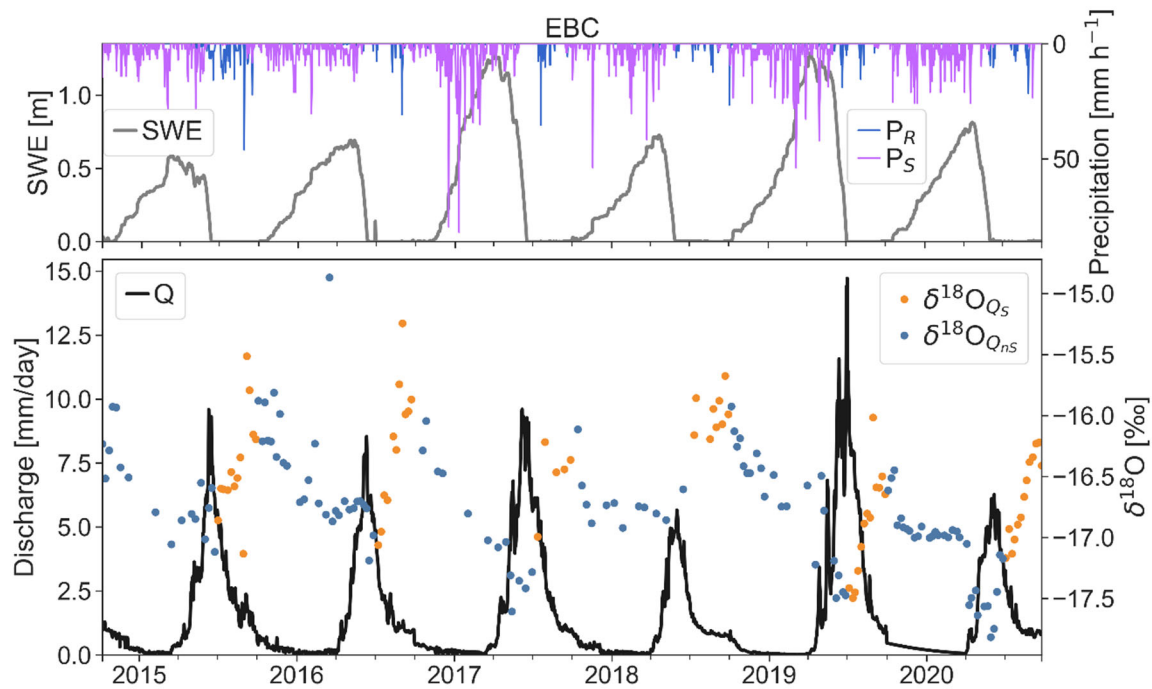
610

611 *Suppl. Fig. 6 Same as in Suppl. Fig. 4, but for the Rock Creek catchment.*



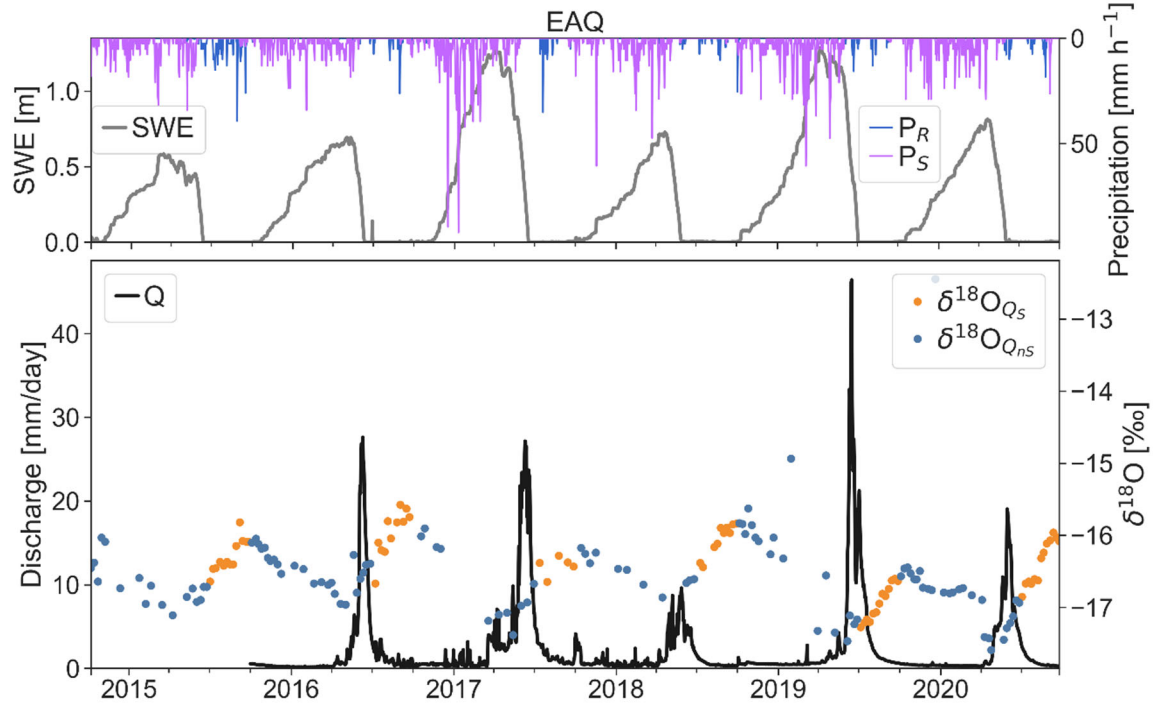
612

613 *Suppl. Fig. 7 Same as in Suppl. Fig. 4, but for the Quigley Creek catchment.*



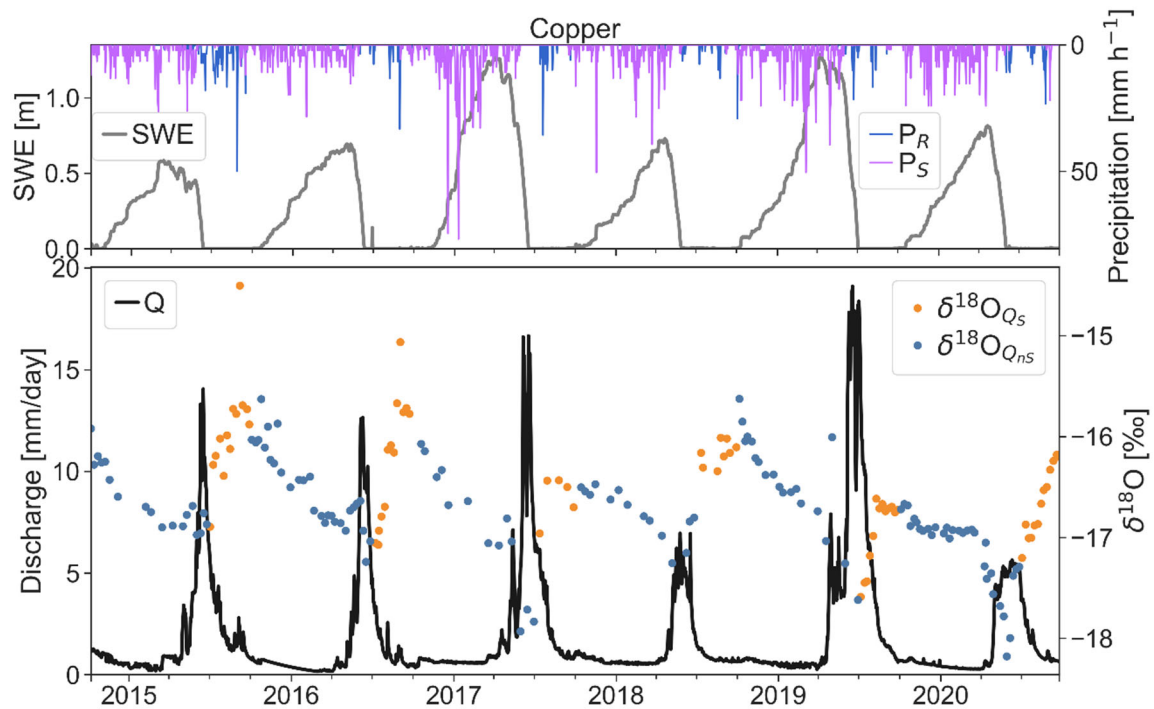
614

615 *Suppl. Fig. 8 Same as in Suppl. Fig. 4, but for the East River catchment below Copper Creek*  
 616 *tributary.*



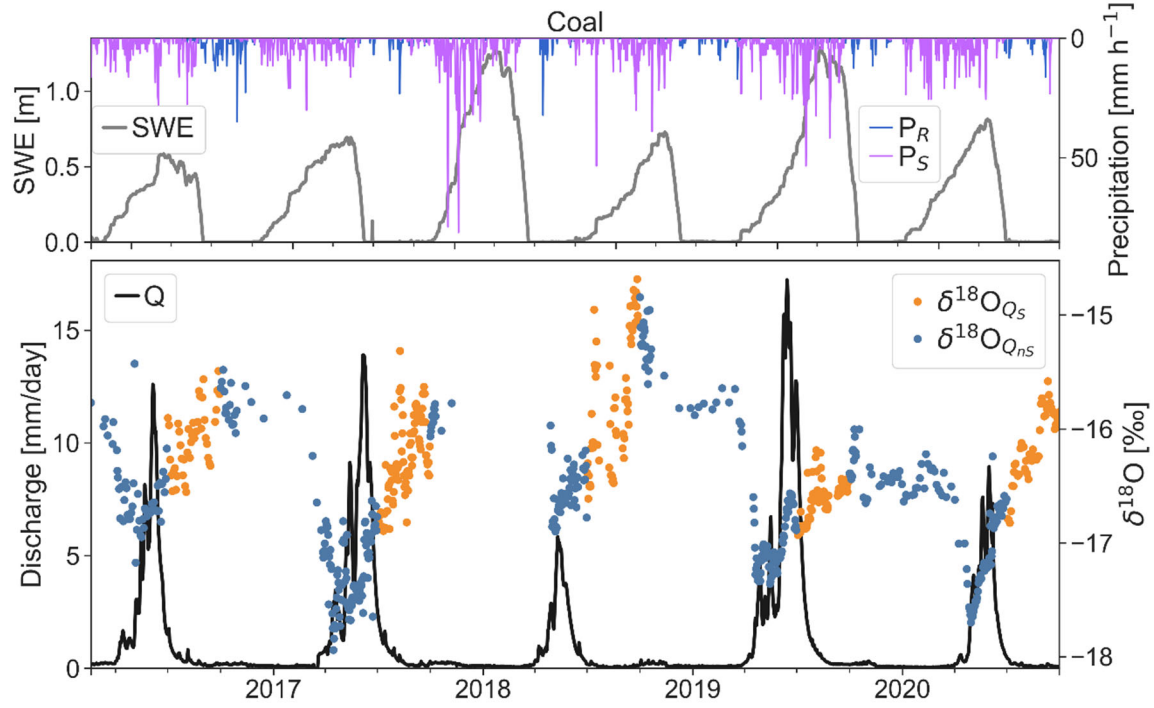
617

618 *Suppl. Fig. 9 Same as in Suppl. Fig. 4, but for the East River catchment above the Quigley*  
 619 *tributary.*



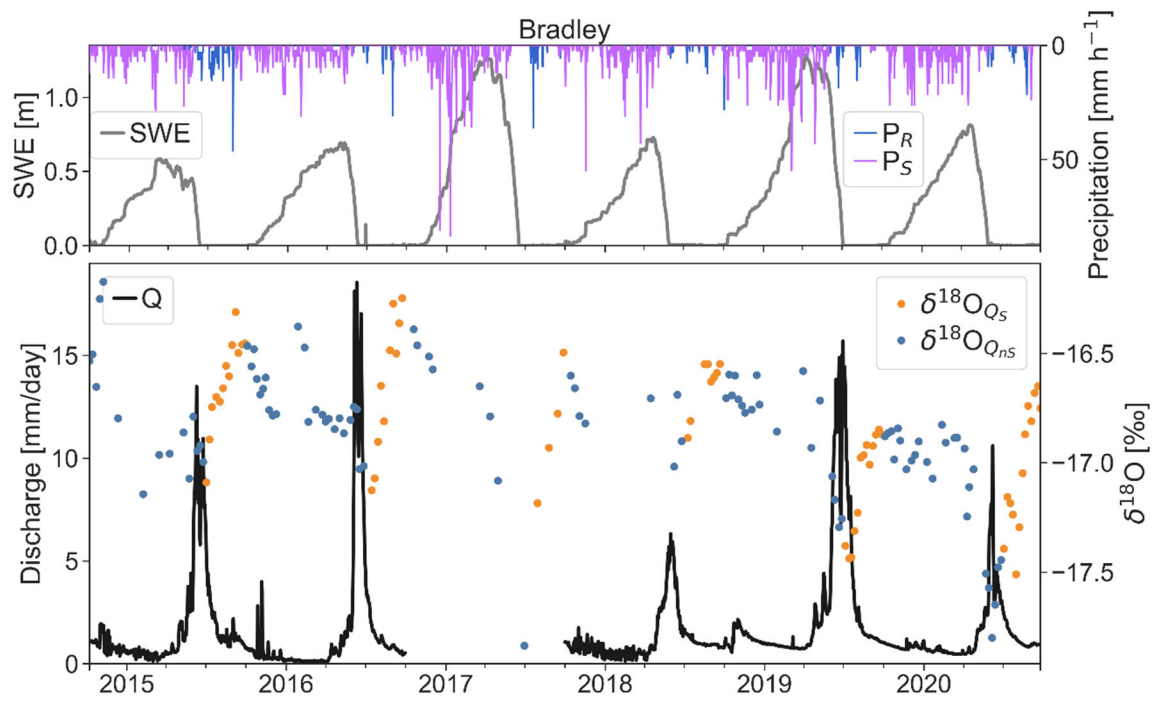
620

621 *Suppl. Fig. 10 Same as in Suppl. Fig. 4, but for the Copper Creek catchment.*



622

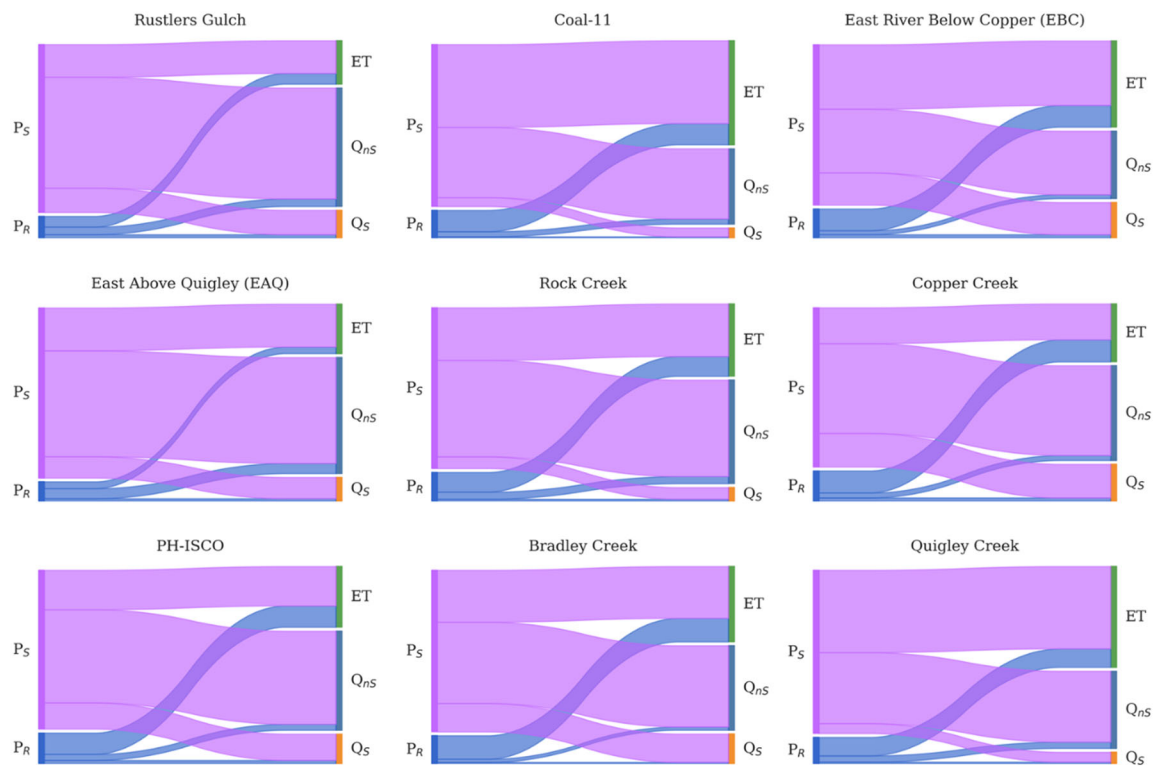
623 *Suppl. Fig. 11 Same as in Suppl. Fig. 4, but for the Coal Creek catchment.*



624

625 *Suppl. Fig. 12 Same as in Suppl. Fig. 4, but for the Bradley Creek catchment.*

626



627

628 *Suppl. Fig. 13 Long-term (2015-2020) isotope mass balance for the nine catchments. Snow ( $P_S$ )*  
 629 *and rain ( $P_R$ ) are split into evapotranspiration ( $ET$ ), non-summer ( $Q_{ns}$ ) and summer season*  
 630 *discharge ( $Q_S$ ) based on endmember splitting analysis. The composition of  $ET$ ,  $Q_{ns}$  and  $Q_S$  with*  
 631 *regard to snow and rain is based on endmember mixing analysis.*

632

*Suppl. Table 1 Catchment specific characteristics: total surface area [km<sup>2</sup>], catchment scale averages of the slope [-], aspect [°], elevation [m a.s.l.], relief [m], drainage density [km/km<sup>2</sup>], topographic wetness index (TWI) [-], share of montane, subalpine, upper subalpine, alpine, Mancos lithology, and barren land as % of total catchment area. EAQ = East River above Quigley, EBC = East River above Copper Creek, PH = Pumphouse. We derived catchment average tree cover density using USGS Landfire at 30 m raster maps (Landfire, 2015, Existing vegetation type and cover layers. U.S. Department of the Interior, Geological Survey. <http://landfire.cr.usgs.gov/viewer>, accessed October 2021) weighing the different forest classes by their given tree density. Alpine > 3750 m; upper subalpine: 3700-3525 m; subalpine: 3525–3000 m, montane: <3000 m.*

|          | Area [km <sup>2</sup> ] | Slope [-] | Aspect [°] | Elevation [m asl] | Relief [m] | DD [km/km <sup>2</sup> ] | TWI [-] | Tree density [%] | Montane [%] | Subalpine [%] | upper Subalpine [%] | Alpine [%] | Mancos [%] | Barren [%] |
|----------|-------------------------|-----------|------------|-------------------|------------|--------------------------|---------|------------------|-------------|---------------|---------------------|------------|------------|------------|
| Quigley  | 2.55                    | 26        | 95         | 3,365             | 911        | 1.47                     | 4.9     | 26               | 2           | 78            | 17                  | 3          | 62         | 23         |
| Rock     | 3.57                    | 19        | 120        | 3,363             | 930        | 1.71                     | 5.2     | 32               | 1           | 86            | 11                  | 2          | 68         | 8          |
| Bradley  | 3.82                    | 26        | 233        | 3,485             | 1,102      | 1.76                     | 4.9     | 20               | 6           | 45            | 30                  | 19         | 1          | 40         |
| EAQ      | 5.27                    | 28        | 130        | 3,333             | 904        | 1.56                     | 5.0     | 24               | 1           | 82            | 15                  | 2          | 70         | 21         |
| Rustlers | 14.78                   | 26        | 191        | 3,475             | 1,118      | 1.75                     | 4.9     | 18               | 1           | 57            | 29                  | 13         | 8          | 23         |
| Copper   | 23.67                   | 29        | 191        | 3,513             | 1,237      | 1.75                     | 4.8     | 14               | 2           | 47            | 31                  | 20         | 1          | 50         |
| Coal     | 52.80                   | 18        | 164        | 3,148             | 1,073      | 1.81                     | 5.3     | 39               | 23          | 72            | 5                   | 0          | 0          | 3.5        |
| EBC      | 69.81                   | 25        | 168        | 3,351             | 1,196      | 1.26                     | 5.0     | 24               | 10          | 63            | 20                  | 7          | 18         | 31         |
| PH       | 84.73                   | 25        | 169        | 3,331             | 1,362      | 1.85                     | 5.0     | 22               | 18          | 53            | 20                  | 9          | 18         | 26         |